Materials Science and Engineering C 68 (2016) 52–58

Contents lists available at ScienceDirect

Materials Science and Engineering C

journal homepage: www.elsevier.com/locate/msec

Impedimetric immunosensor for detection of cardiovascular disorder risk biomarker

Raju Khan [a,*], Mintu Pal [b], Alexey V. Kuzikov [c], Tanya Bulko [c], Elena V. Suprun [c], Victoria V. Shumyantseva [c]

[a] Analytical Chemistry Division, CSIR-North East Institute of Science & Technology, Academy of Scientific and Innovative Research, Jorhat 785006, Assam, India
[b] Biotechnology Division, CSIR-North East Institute of Science & Technology, Academy of Scientific and Innovative Research, Jorhat 785006, Assam, India
[c] Institute of Biomedical Chemistry, Pogodinskaya Street, 10, Moscow 119121, Russia

ARTICLE INFO

Article history:
Received 27 February 2016
Received in revised form 20 May 2016
Accepted 23 May 2016
Available online 24 May 2016

Keywords:
Cardiovascular disease
Myoglobin
Immunosensors
Electrochemical impedance spectroscopy
Screen-printed multiwalled carbon nanotubes electrode

ABSTRACT

We report the construction and characterization of a novel, level free impedimetric immunosensor for rapid, sensitive and selective detection of myoglobin (Mb). Monoclonal *anti*-myoglobin (*anti*-Mb-IgG) antibody was immobilized on screen-printed multiwalled carbon nanotubes electrode for signal amplification without the need of natural enzymes. The fabrication of resulting immunosensor was extensively characterized by using scanning electron microscopy (SEM), fourier transform infrared (FT-IR) spectroscopy, cyclic voltammetry (CV), differential pulse voltammetry (DPV) and electrochemical impedance spectroscopy (EIS). Electrochemical impedance spectroscopy (EIS) technique offered a linear detection range (0.1–90 ng mL^{-1}) of myoglobin with sensitivity of 0.74 kΩ ng mL^{-1} (correlation coefficient, $R^2 = 0.97$) and detection limit of 0.08 ng mL^{-1} (S/N = 3). The mean percentage recovery of Mb in serum samples using this working biosensor is 97.33%. Furthermore, the proposed strategy can be a promising alternative for detection of Mb related cardiovascular disorders.

1. Introduction

The cardiovascular disease (CVD) is one of the major threats to global health, giving utmost importance to the diagnosis and prevention of acute myocardial infarction. Cardiac biomarkers in blood sample provide an effective way to diagnose the illness, making the importance of biomarkers as a predictor of morbidity and mortality. Biomarkers for the detection of cardiac infarction include myoglobin (Mb), creatine kinase MB (CK-MB), cardiac troponins (cTn), and myeloperoxidase (MPO) [1,2]. Myoglobin is found in mammalian skeleton and muscle tissues, regulating the storage and diffusion of oxygen in heart and skeletal muscles. Myoglobin is a sensitive marker for muscle injury, a potential code for heart attack in patients with chest pain [3]. Among the above-mentioned biomarkers, Mb is one of the very early markers, which up-regulated after acute myocardial infarction (AMI). Therefore, a highly efficient, rapid, and sensitive detection method are urgently needed for measuring myoglobin concentration at low levels. In recent studies, various methods such as the electrochemical [4–9], fluorescent [10], and colorimetric have been developed to detect myoglobin [11]. In addition, conventional enzyme-linked immunosorbent assay (ELISA) and radioimmunoassay (RIA) have developed for the diagnostic purposes of AMI [12,13]. However, these approaches have certain demerits; include multistep processing of samples, low sensitivity, and the overall high cost. In this regard, biosensors for protein detection are very efficient and cost-effective with high sensitivity and selectivity [14]. In the recent decades, scientists are focussing in finding out specific good biocompatible material to improve the behaviour of biosensors [15]. One such finding is the immobilization of biomolecules in designer-made nanoscale structures, which can significantly improve the performance of biocatalytic processes. Therefore, nanomaterials with their specific physicochemical properties, such as high surface area, excellent biocompatibility, good thermal and chemical stability [16] are the promising material in the field of electrochemical biosensors. A nanomaterial with special structures facilitates the transfer of electron between the electrode and immobilized proteins [17]. For the development of biosensors various nanomaterials used as a substrates, such as carbon nanotubes (CNT) offer a wide variety of advantages including high electrode surface area and good electrical conductivity [18,19]. Furthermore, recent studies have demonstrated that CNT can enhance the electrochemical reactivity of biomolecules and promote electron transfer reactions [20,21]. Screen-printed carbon nanotubes electrodes (SPEs) have certain advantages such as simple and low cost fabrication and conveniently applied for the detection of biomolecules [22,23]. Among the detection techniques, electrochemical approaches such as cyclic voltammetry (CV) and electrochemical impedance spectroscopy (EIS) have been widely used for the real-time monitoring of biomolecule interaction such as protein, nucleic acid, etc. in contact with the sensor electrode surface. EIS have shown great potential for label-free

* Corresponding author at: Analytical Chemistry Division, CSIR-North East Institute of Science & Technology, Jorhat 785006, Assam, India.
E-mail address: khan.raju@gmail.com (R. Khan).

http://dx.doi.org/10.1016/j.msec.2016.05.107
0928-4931/

detection, simplifying the molecular recognition process and enhancing the sensitivity [24–26]. However, no attempts have been made towards the development of myoglobin sensor based on screen- printed electrode containing Multi-Walled Carbon Nanotubes (MWCNTs). Therefore, the goal of this study is to develop a novel impedimetric biosensor for the detection of myoglobin based on screen-printed electrode containing MWCNTs.

In the present study, we have demonstrated a simple, immunosensor based-electrochemical impedance method to detect myoglobin onto the immobilized *anti*-Mb-IgG using screen-printed electrode containing multiwalled carbon nanotubes. Overall, our studies revealed that the developed Mb-specific immunobiosensor is a very effective with high sensitivity, specificity with low detection limit of 0.08 ng mL^{-1} over the current studies on different types of biosensor.

2. Experimental section

2.1. Reagents

Myoglobin from equine skeletal muscle, monoclonal *anti*-myoglobin antibody produced in mouse (M7773) from Sigma-Aldrich, USA. Sodium phosphate dibasic (Na_2HPO_4, purity 99.95%) and sodium phosphate mono basic ($NaH_2PO_4 \cdot H_2O$, purity 98%) were procured from Sigma-Aldrich, USA.

2.2. Electrochemical measurements

Cyclic voltammetry and electrochemical impedance spectroscopy measurements were performed using a potentiostat/galvanostat/ZRA (Gamry Reference 3000, USA) with Gamry Echem Analyst Software. The electrochemical experiments were carried out using the screen-printed electrodes with multi-walled carbon nanotubes (SPEs-MWCNTs) and *anti*-myoglobin antibodies immobilized onto the SPEs-MWCNTs (SPEs-MWCNTs-*anti*-Mb-IgG), followed by blocking with bovine serum albumin (SPEs-MWCNTs-*anti*-Mb-IgG-BSA) to avoid non-specific binding of antigen that has been considered as an effective working electrode for the subsequent studies of this work. In our experiments, the commercial screen-printed electrode substrates (DRP-110CNT, DropSens; Asturias, Spain, www.dropsens.com) with 4.0-mm diameter multiwalled CNT working electrode, carbon ink counter electrode, and an integrated silver pseudo-reference electrode were performed at ambient temperature (25.0 ± 1.0 °C). The structural characterization of SPEs-MWCNTs and SPEs-MWCNTs-*anti*-Mb-IgG-BSA were done by SEM (Hitachi, model S-5500). The functionality of SPEs-MWCNTs and SPEs-MWCNTs-*anti*-Mb-IgG-BSA immobilization was confirmed by a FT-IR spectrophotometer (Spectrum 100 with software version CPU32).

The developed SPEs-MWCNTs, SPEs-MWCNTs-*anti*-Mb-IgG and SPEs-MWCNTs-*anti*-Mb-IgG-BSA electrodes were characterized electrochemically through CV and EIS techniques prior to their use in myoglobin detection. In cyclic voltammetry and electrochemical impedance spectroscopy, decreased peak current was observed with the increased in charge resistance transfer [10,11]. Herein, the CV data were recorded between −0.3 V to 0.9 V versus SPEs-MWCNTs with a scan rate of 10 mVs^{-1} in 50 mM phosphate buffer saline (PBS), pH 7.40 ± 0.01 with 5 mM $[Fe(CN)_6]^{3-/4-}$. The electrochemical impedance spectroscopy has studied at 0.1 Hz to 100 kHz at open circuit potential.

2.3. Fabrication of antibody based electrochemical Mb immunosensor

The immunoelectrode (SPEs-MWCNTs-*anti*-Mb-IgG) for detection of myoglobin was prepared by immobilizing monoclonal *anti*-myoglobin antibody (5 μL of 105 ng mL^{-1} monoclonal *anti*-Mb-IgG stock solution in phosphate buffer, pH 7.40 ± 0.01) onto the SPEs-MWCNTs electrode by adsorption technique and incubated at 4 °C overnight. The conditions for the immobilization of the antibodies were selected based on our previous studies [5,26,27]. After capturing the antibodies onto the electrode, subsequent washed with PBS to remove the unbounded antibodies, followed by blocking step with 1% BSA in PBS. The electrode was stored at 4 °C in pH 7.40 ± 0.01 phosphate buffer solution for subsequent experiments. The schematic illustration for fabrication of the immunosensor and the biochemical reaction of IgG with myoglobin at the SPEs-MWCNTs surface has been shown in Fig. 1.

2.4. Fourier-transform-infrared spectra analysis

FTIR (Spectrum 100 with software version CPU32 spectrometer) was used for the confirmation of exposed carboxylated group needed for immobilization and validation of captured antibodies onto the MWCNTs electrode.

2.5. Scanning electron microscopy

Scanning Electron Microscope (Hitachi, model S-5500) was used for the characterization of surface morphology of SPEs-MWCNTs, SPEs-MWCNTs-*anti*-Mb-IgG and SPEs-MWCNTs-*anti*-Mb-IgG-BSA electrodes.

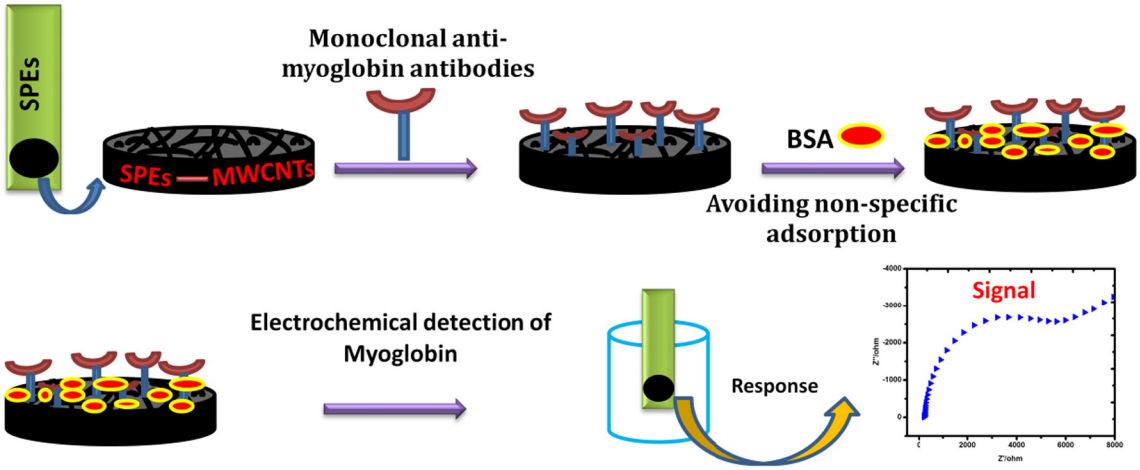

Fig. 1. Schematic illustration of the fabrication process for an electrochemical biosensor (SPEs-MWCNTs) based on *anti*-myoglobin antibody immobilized on MWCNTs electrode.

2.6. Electrochemical detection of myoglobin

For the detection of Mb, we prepared a stock solution of 1 mg mL^{-1} in freshly prepared 50 mM PBS (pH 7.40 ± 0.01), followed by the working concentration of Mb prepared by appropriate dilutions of the stock solution in PBS containing 5 mM $[Fe(CN)_6]^{3-/4-}$. For the interference assessment, the working biosensor was used to detect Mb in human serum. The human serum was diluted 10 times using PBS. Subsequently, the Mb with serum samples were prepared by adding Mb in 1:10 diluted serum samples.

3. Results and discussion

3.1. Electrochemical analysis by CV

The SPEs-MWCNTs, SPEs-MWCNTs-*anti*-Mb-IgG and SPEs-MWCNTs-*anti*-Mb-IgG-BSA electrodes for detection of myoglobin were characterized by cyclic voltammetry (CV). Cyclic voltammograms studies revealed the variation of scan rate from 5 mVs^{-1} to 100 mVs^{-1} recorded between −0.3 V to 0.9 V for (a) SPEs-MWCNTs (b) SPEs-MWCNTs-*anti*-Mb-IgG and (c) SPEs-MWCNTs-*anti*-Mb-IgG-BSA electrodes in 50 mM PBS, pH 7.40 ± 0.01 containing 5 mM $[Fe(CN)_6]^{3-/4-}$, indicating the cathodic and anodic peak currents simultaneously increases as shown in Fig. 2 (I, II & III). Cyclic voltammograms obtained at different scanning rates indicate that the value of ΔE_p ($\Delta E_p = E_{pa} - E_{pc}$) increases at higher rates as shown in Fig. 2 (IV), signifying that the slow kinetics of electron transfer on the electrode surface because of the electrode have considerable resistance.

To validate the capturing antibodies onto the electrode, we checked relative variation of current in cyclic voltammograms at constant 10 mVs^{-1} scan rate in PBS (50 mM, pH 7.40 ± 0.01) containing 5 mM $[Fe(CN)_6]^{3-/4-}$ as shown in Fig. 3. After the immobilization of *anti*-Mb-IgG, decreases the peak current as shown in Fig. 3 (I), curve (b) and substantial blockage of the immunoelectrode with BSA slightly current decreased as in curve (c). This signifies the successful capturing of *anti*-Mb-IgG and nonspecific BSA on the electrode surface. The correlation of the peak current, I_{pa} and I_{pc}, against $\upsilon^{1/2}$ (υ is the scan rate) is linear, as shown in Fig. 3 (II) & (III), which is very similar to a diffusion controlled process. Diffusion coefficient is calculated from Randles-Sevcik equation as,

$$i_p = 0.04463\ nF(nFD/RT)^{1/2}AC\upsilon^{1/2}$$

where, i_p is the peak current, n is the number of electron, F is Faraday Constant (96,500), T is temperature in Kelvin, R is the gas constant, A is surface area of the working electrode, D is the diffusion coefficient of the electroactive species, C is the bulk concentration of the electroactive species and υ is the scan rate of voltammograms. In the graph linear response with the square scan rate observed and is a diffusion controlled process where slope of peak current with square root of scan rate [$d(I)/d(\upsilon^{1/2})$ is proportional to $D^{1/2}$] depends on diffusion coefficient. The drastic decrease of slope after immobilization of *anti*-Mb-IgG and blocking of BSA from 7.8×10^{-6} μA (for only bare electrode) to 4.7×10^{-6} & 3.9×10^{-6} μA respectively, with the equation $y = a + b * x$; $R^2 = 0.99$; overall indicting the strong binding of *anti*-Mb-IgG to SPEs-MWCNTs onto the electrode. Consequently, we have also characterized the capturing antibody on the electrode by EIS and FTIR analysis. To make confirm the specificity to myoglobin, we used Mb free buffer sample as negative control. CV was performed in a potential range of −0.3 V to 0.9 V at a scan rate of 10 mVs^{-1} 20 numbers of cycles to monitoring the reproducibility of the immunosensor.

3.2. Electrochemical analysis by EIS

To confirm the characterization of resulting immunosensor, we have used electrochemical impedance spectroscopy (EIS). Results have

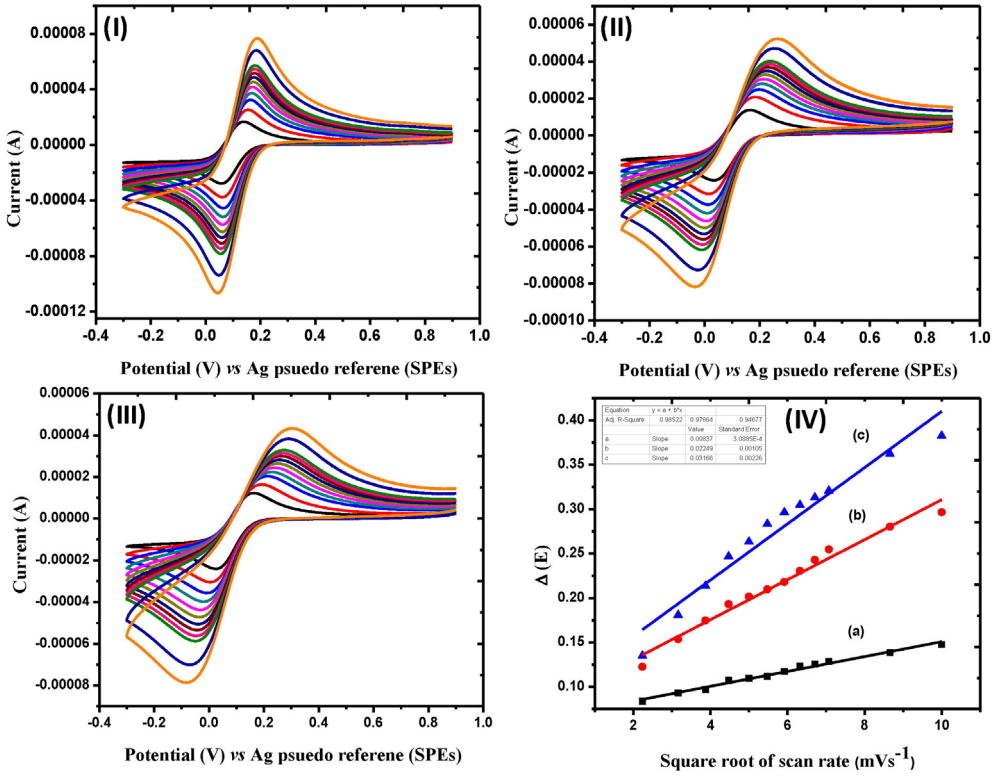

Fig. 2. Cyclic voltammograms of (I) SPEs-MWCNTs; (II) SPEs-MWCNTs-*anti*-Mb-IgG; (III) SPEs-MWCNTs-*anti*-Mb-IgG-BSA electrodes in PBS (50 mM, pH 7.4) containing 5 mM $[Fe(CN)_6]^{3-/4-}$ at scan rate from 05 mVs^{-1} to 100 mVs^{-1} and (IV) Difference between cathodic (E_{pc}) and anodic peaks (E_{pa}).

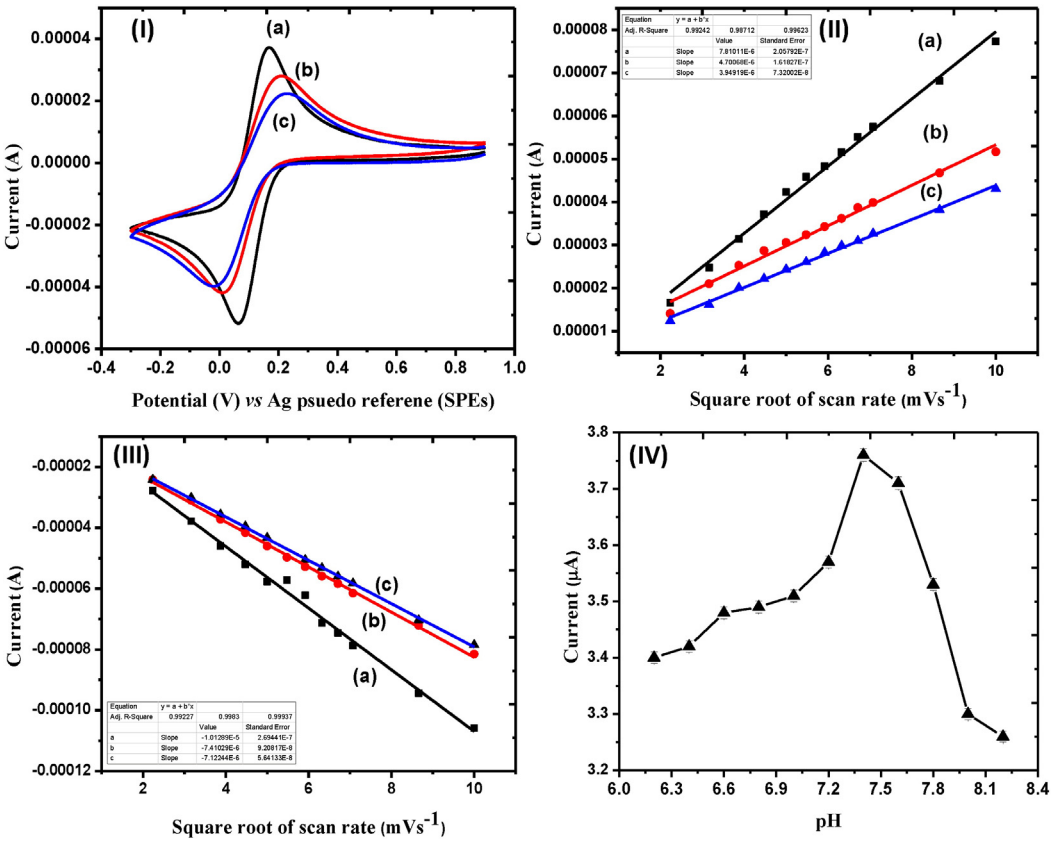

Fig. 3. (I) Cyclic voltammograms of (a) SPEs-MWCNTs; (b) SPEs-MWCNTs-*anti*-Mb-IgG; (c) SPEs-MWCNTs-*anti*-Mb-IgG-BSA electrodes in PBS (50 mM, pH 7.4) containing 5 mM $[Fe(CN)_6]^{3-/4-}$ at constant scan rate 10 mVs^{-1}; (II) and (III) the dependence of reduction and oxidation peak current with square root of scan rate; (IV) Effect of pH on the differential pulse voltammetric response of the immunosensor at 5 ng mL^{-1} myoglobin.

shown that two types of impedance are produced, such as real portion (Z_{real}) for the indication of characteristic capacitance and the imaginary part ($-Z_{imag}$) for resistance elements of the electrode-electrolyte interface (Fig. 4); that follows a complex representation, $Z(\omega) = Z'(\omega) + jZ''(\omega)$ [28–30]. Fig. 4 (I) showed the Nyquist plots recorded for (a) bare SPEs-MWCNTs, (b) SPEs-MWCNTs-*anti*-Mb-IgG and (iii) SPEs-MWCNTs-*anti*-Mb-IgG-BSA electrodes in 50 mM PBS of pH 7.4 ± 0.01 containing 5 mM $Fe(CN)_6^{4-}/Fe(CN)_6^{3-}$ solution. On the other hand, the calculated higher value of electrical double layer (C_d) of SPEs-MWCNTs interface is probably nanotube provided higher surface of the electrode as shown in the Table 1 and Fig. 4 (II) & (III). As expected, the SPEs-MWCNTs exhibited the lowest charge transfer resistance (R_{CT}), 1.32 kΩ, which is a much smaller value than that of the captured antibodies ((R_{CT}) = 7.94 kΩ) and BSA (6.22 kΩ) treated electrodes, indicating the efficient immobilization of antibody to the electrode. The surface concentration of the immunosensors was calculated from the plot of current versus potential by Brown-Anson Model using $I_p = n^2F^2I^*A\upsilon/4RT$ equation [31]. In this equation, n is the number of electrons transferred, F is the Faraday constant, I* is the surface concentration (mol mm^3) of the resulting immunosensor, A is the surface area (4 mm^2) of the electrode, υ is the scan rate (10 mVs^{-1}), R is the gas constant and T is the absolute temperature. The effective surface concentration of the antibodies on the electrode was found to be 2.69×10^{-5} mol mm^3.

3.3. Fourier transform infrared (FTIR) spectroscopy studies

To further confirm the immobilization of monoclonal *anti*-myoglobin antibody on the electrode surface, we have used FTIR spectroscopy analysis with scanned between 400-4000 cm^{-1}. As a result, we found a broad peak line at 3424 cm^{-1} might be due to the presence of intermolecular hydrogen bonding, that refers to the O-H stretch of the hydroxyl group, indicating the oscillation of carboxyl groups as shown in Fig. 4 (IV), curve (a). It is known that the peak at 1634 cm^{-1} is associated with the stretching of the carbon nanotube backbone [32,33]. In the curve (b), after *anti*-Mb-IgG attachment onto the SPEs-MWCNTs, a new strong absorbance 1653 cm^{-1} observed that indicates the –COOH group on MWCNTs reacted with the amine group on the antibodies to form amide bond (−CONH–). The absorbance signal at 614 cm^{-1}, and the peak at 578 cm^{-1} can be assigned to ring deformation and out of plane C-H bending vibrations respectively.

3.4. Scanning Electron Microscopy studies

To further validate the effective immobilization of antibody on the electrode, we have performed SEM analysis. At lower magnification, images shown bunch of nanotubes on electrodes surface; whereas at higher magnification, it is clearly shown the morphology of nanotubes with globules like structure (radius 9.5 ± 0.5 nm) on the resulting electrode surface as shown in Fig. 5 (I–II). Successful adsorption of the *anti*-Mb-IgGs was observed on the surface of SPEs-MWCNTs electrode as shown in Fig. 5 (III), as well as the application of blocking agent BSA was also observed in Fig. 5 (IV). With careful observation, we found there is no huge difference superficially between antibody immobilization and antibody immobilization followed by blocking with BSA as shown in Fig. 5 (V) & (VI) respectively; in accordance with our electrochemistry studies, we observed small changes of R_{CT} values in the EIS measurement.

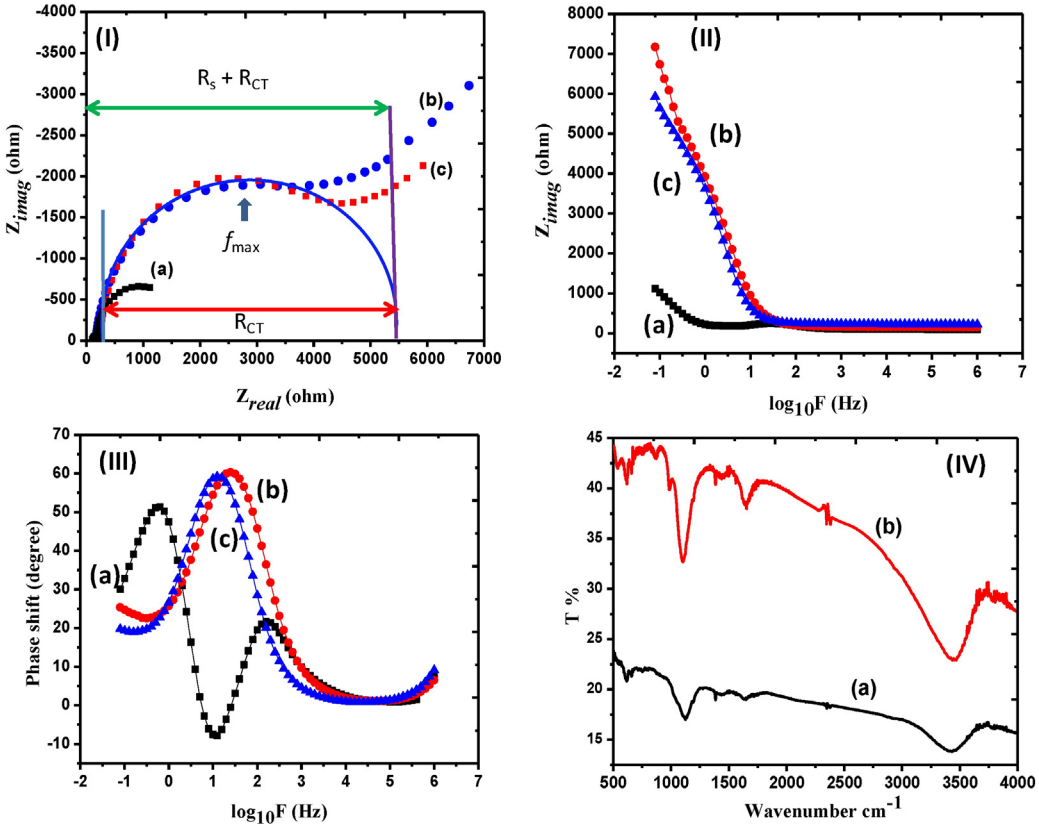

Fig. 4. (I) EIS Nyquist plots of (a) SPEs-MWCNTs (b) SPEs-MWCNTs-*anti*-Mb-IgG and (c) SPEs-MWCNTs-*anti*-Mb-IgG-BSA electrodes in PBS (50 mM, pH 7.4) containing 5 mM $[Fe(CN)_6]^{3-/4-}$. (II) Bode plots for (a) SPEs-MWCNTs (b) SPEs-MWCNTs-*anti*-Mb-IgG and (c) SPEs-MWCNTs-*anti*-Mb-IgG-BSA. (III) Phase shift in bode plots for (a) SPEs-MWCNTs (b) SPEs-MWCNTs-*anti*-Mb-IgG and (c) SPEs-MWCNTs-*anti*-Mb-IgG-BSA. (IV) FTIR spectra of (a) SPEs-MWCNTs and (b) SPEs-MWCNTs-*anti*-Mb-IgG-BSA.

3.5. Electrochemical analysis by DPV

To optimize the proper pH condition for the experiment, we used differential pulse voltammetry (DPV) to detect the analyte (Mb) onto the antibody immobilized electrode. SPEs-MWCNTs-*anti*-Mb-IgG-BSA immunosensor in PBS (pH range 6.2–8.2 ± 0.01) was used for optimization of Mb as an analyte on the electrode using DPV at potential from −0.3 V to 0.9 V, pulse size 85 mV and step size of 4 mV. As a result, we found a single well-defined oxidation peak at −0.018 V. In the case of *anti*-Mb-IgG electrode, the highest differential pulse voltammetry peaks current was obtained at pH 7.40 ± 0.01, suggesting the optimal pH for best sensitivity for the studies as shown in Fig. 3 (IV), the similar strategy has been used for the immobilization of antibodies (*anti*-troponin-I) on carbon nanofiber based nanoelectrodes [34].

3.6. Electrochemical detection of Mb

The sensitivity of the detection platform was studied through EIS measurements using different concentrations of myoglobin under the optimized working conditions as shown in Fig. 6. The Nyquist plots shows that R_{CT} is suitable to evaluate concentration dependent characteristics. In the Nyquist plots diameter of the circle notably increases with increasing concentration of myoglobin. This possibly can be due to the ability of more analytes binding to the immunosensor at higher concentration of myoglobin. Calibration graph shows the impedimetric responses of the sensor electrode for various concentrations of myoglobin (0, 0.1, 0.5. 1, 5, 10, 30, 50, 70 and 90 ng mL^{-1}); with sensitivity of 0.74 kΩ ng mL^{-1}. The detection limit of the immunosensor is 0.08 ng mL^{-1} was very low compared to other recently published studies as given in Table 2. The stability of the electrode was determined by continuously monitoring the impedance response at 0.1 ng mL^{-1} myoglobin concentration for one-day interval for 25 days at 25 °C and stored at 4 °C, and found 91% of its initial signal under the identical experimental conditions.

3.7. Validation and recovery characteristics of Mb immunosensor in serum samples

To check for the existence of interferences of Mb in serums, we performed with a standard method of recovery percentage, which is 97.33% as shown in Table 3, indicating that the interferences of other components in the serum is very minimum with the precision of our experimental results. In this study, we obtained RSD values for Mb in PBS and in serum were 0.161% and 1.50% respectively. Moreover, it has shown considerable repeatability and reproducibility data, confirming a promising alternative method for the direct determination of Mb in biological fluids with minimum interferences.

4. Conclusion

We designed and developed an impedimetric myoglobin immunosensor for the diagnosis of myocardial infarction based on multiwalled CNT and myoglobin specific immobilizing monoclonal

Table 1
R_{CT}, C_D and Phase Shift (Φ) values of SPEs-MWCNTs, SPEs-MWCNTs-*anti*-Mb-IgG and SPEs-MWCNTs-*anti*-Mb-IgG-BSA.

Matrix	R_{CT} (kΩ)	C_d (F)	Phase shift (Φ)
SPEs-MWCNTs	1.32	476	−19.51
SPEs-MWCNTs-*anti*-Mb-IgG	7.94	2.48	−37.69
SPEs-MWCNTs-*anti*-Mb-IgG-BSA	6.22	2.52	−40.40

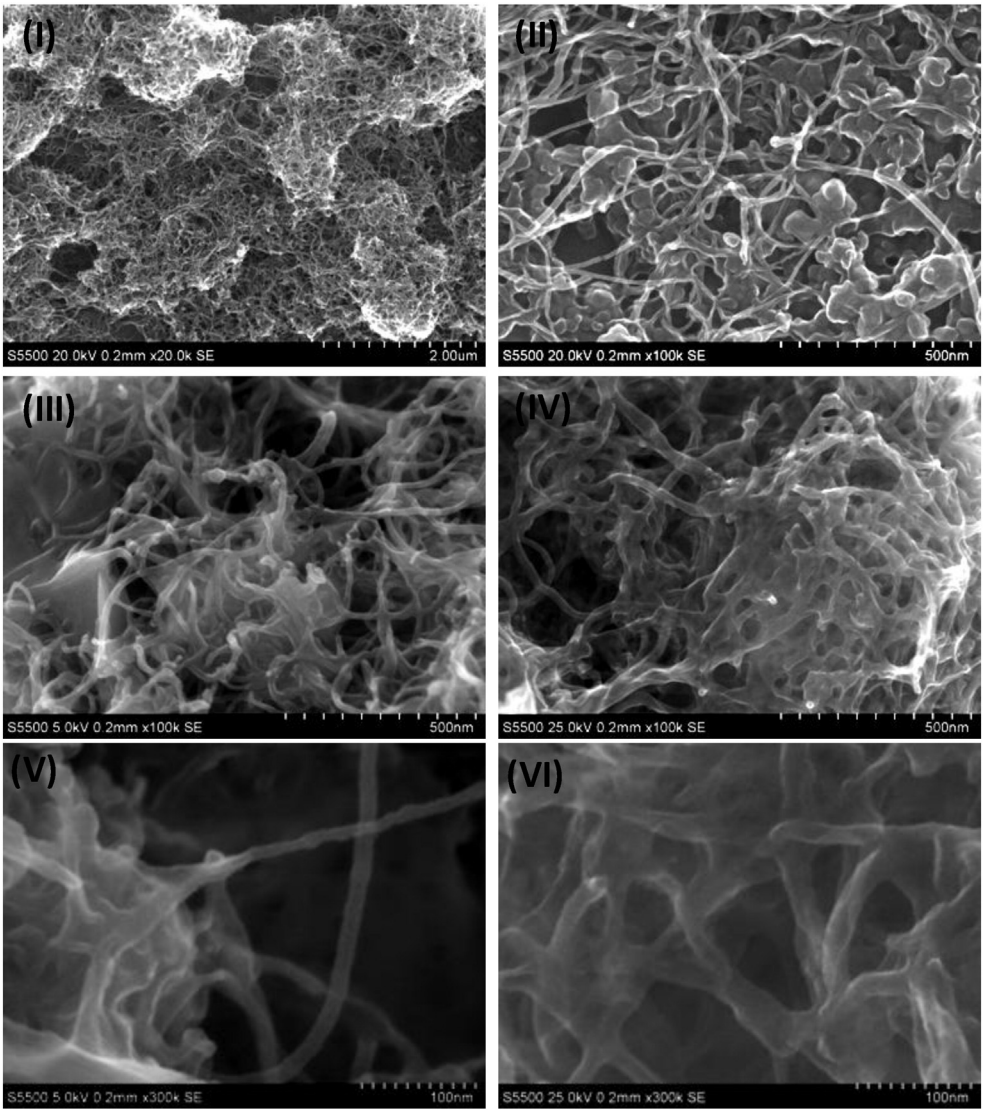

Fig. 5. SEM micrograph of (I & II) SPEs-MWCNTs at lower and higher magnification; (III) *anti*-Mb-IgG on SPEs-MWCNTs after immobilization; (IV) *anti*-Mb-IgG on SPEs-MWCNTs after immobilization followed by the application of blocking agent BSA; (V) *anti*-Mb-IgG on SPEs-MWCNTs after immobilization at higher magnification and (VI) *anti*-Mb-IgG on SPEs-MWCNTs after immobilization followed by blocking with BSA at higher magnification.

antibody, which employs to interact with the analyte Mb proteins. FT-IR, CV, DPV, EIS and SEM techniques were used to characterize each stage involved in fabricating the CNT electrode, capturing of antibody, and the captured antibody-myoglobin interaction at the electrode surface. The resulting fabricated electrochemical immunosensor is highly specific and sensitive of 0.74 kΩ ng mL^{-1}, with a detection limit of 0.08 ng mL^{-1}. This electrochemical immunosensor may provide an efficient platform for the early

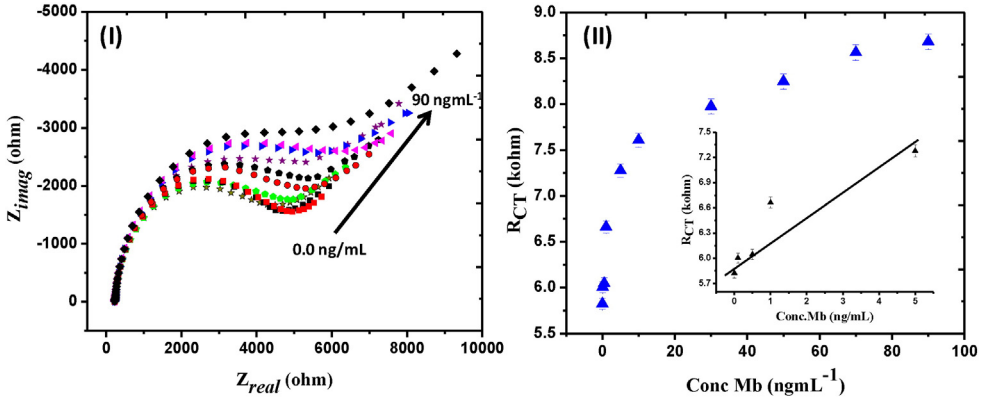

Fig. 6. (I) Nyquist plots of SPEs-MWCNTs-*anti*-Mb-IgG-BSA Immunosensor with bare electrode and different concentrations of myoglobin from 0.1 to 90 ng mL^{-1}. (II) Calibration plots showing R_{CT} for different concentrations of myoglobin from 0.1 to 90 ng mL^{-1} and inset showing the calibration plot of myoglobin from 0.1 to 5 ng mL^{-1}.

Table 2
Summary of the various detection methods reported in the literature, along with their important parameters.

Device	Limit of detection	Detection method	Reference
Fiber-optic immunosensor	83 μg/L	Fluorescence intensity detection	[35]
Triage cardiac panel (Biosite)	Quantitative measurements above clinical baseline concentrations	Fluorescence intensity detection	[36]
Alpha Dx (First Medical Inc.)	5 μg/mL	Fluorescence intensity detection	[37]
Polyaniline (PANI) nanowire-based biosensor	1.4 ng mL^{-1}	Conductance measurement	[4]
The MIP/Au-SPE devices	2.25 μg/mL	Electrochemical impedance response	[38]
Aptamer based electrochemical biosensor	10 pM	Electrochemical detection	[39]
Au electrode immunosensor	5.2 ng mL^{-1}	Electrochemical impedance response	[28]
SPEs-MWCNTs-*anti*-Mb-IgG-BSA	0.08 ng mL^{-1}	Electrochemical impedance response	Present work

Table 3
Percentage recovery of Mb in serum samples based on impedimetric immunosensor (n = 5).

Concentration	R_{CT} (kΩ) (n = 5)	Average	SD	RSD %
Mb in PBS (0.5 ng mL^{-1})	6.046, 6.058, 6.031, 6.041, 6.042	6.043	0.0097	0.161
Mb in Serum (0.5 ng mL^{-1})	6.023, 5.826, 5.852, 5.911, 5.801	5.882	0.0884	1.50
Recovery = 97.33%				

detection of serum myoglobin levels in clinical samples and point-of-care diagnosis of myocardial infarction.

Acknowledgments

We are grateful to Director, CSIR-NEIST, Jorhat, Assam, India for providing the experimental facilities. Authors are grateful to the Department of Science and Technology (DST), Government of India, for financial support under DST-RFBR, Project Sanctioned No. INT/RUS/RFBR/P-153; SERB-DST SB/S2/RJN-087/2014 and Project of Russian Ministry of Science and Education No 14.576.21.0045 (Unique Identifier RFMEF157614X0045).

References

[1] B. McDonnell, S. Hearty, P. Leonard, R. O'Kennedy, Clin. Biochem. 42 (2009) 549.
[2] U. Friess, M. Stark, Anal. Bioanal. Chem. 393 (2009) 1453.
[3] M. Weber, M. Rau, K. Madlener, A. Elsaesser, D. Bankovic, V. Mitrovic, C. Hamm, Clin. Biochem. 38 (2005) 1027.
[4] I. Lee, X. Luo, X.T. Cui, M. Yun, Biosens. Bioelectron. 26 (2011) 3297.
[5] E. Suprun, T. Bulko, A. Lisitsa, O. Gnedenko, A. Ivanov, V. Shumyantseva, A. Archakov, Biosens. Bioelectron. 25 (7) (2010) 1694.
[6] V.V. Shumyantseva, T.V. Bulko, M.Y. Vagin, E.V. Suprun, A.I. Archakov, Biochem. (Mosc) Suppl. Ser. B. Biomed. Chem. 4 (3) (2010) 237.
[7] E.V. Suprun, A.L. Shilovskaya, A.V. Lisitsa, T.V. Bulko, V.V. Shumyantseva, A.I. Archakov, Electroanalysis 23 (2011) 1051.
[8] E.V. Suprun, A.A. Saveliev, G.A. Evtugyn, A.V. Lisitsa, T.V. Bulko, V.V. Shumyantseva, A.I. Archakov, Biosens. Bioelectron. 33 (2012) 158.
[9] A.A. Shumkov, E.V. Suprun, S.Z. Shatinina, A.V. Lisitsa, V.V. Shumyantseva, A.I. Archakov, BioNanoScience 3 (2013) 216.
[10] F. Darain, P. Yager, K.L. Gan, S.C. Tjin, Biosens. Bioelectron. 24 (2009) 1744.
[11] X. Zhang, X. Kong, W. Fan, X. Du, Langmuir 27 (2011) 6504.
[12] J. Wang, A. Ibanez, M.P. Chatrathi, A. Escarpa, Anal. Chem. 73 (2001) 5323.
[13] F.S. Apple, A. Falahati, P.R. Paulsen, E.A. Miller, S.W. Sharkey, Clin. Chem. 43 (1997) 2047.
[14] T. Vo-Dinh, B.J. Cullum, Anal. Chem. 366 (2000) 540.
[15] M.H. Freeman, J.R. Hall, M.C. Leopold, Anal. Chem. 85 (2013) 4057.
[16] P. Martin, S. Samuel, I. Izumi, J. Tang, Sensors Actuators B 123 (2007) 1195.
[17] Y.H. Xiao, C.M. Li, Electroanalysis 20 (2008) 648.
[18] J. Oh, Y.W. Chang, H.J. Kim, S. Yoo, D.J. Kim, S. Im, Y.J. Park, D. Kim, K.H. Yoo, Nano Lett. 10 (2010) 2755.
[19] X.W. Liu, Y.X. Huang, X.F. Sun, G.P. Sheng, F. Zhao, S.G. Wang, H.Q. Yu, ACS Appl. Mater. Interfaces 6 (2014) 8158.
[20] K. Besteman, J.O. Lee, F.G.M. Wiertz, H.A. Heering, C. Dekker, Nano Lett. 3 (2003) 6.
[21] Y. Lin, F. Lu, Y. Tu, Z. Ren, Nano Lett. 4 (2004) 2.
[22] J. Wang, M. Musameh, Analyst 129 (1) (2004) 1.
[23] M.H. Chin, H. Wu, J.C. Chen, G. Muthuraman, J.M. Zen, Electroanalysis 19 (22) (2007) 2301.
[24] F. Patolsky, A. Lichtenstein, I. Willner, J. Am. Chem. Soc. 123 (2001) 5194.
[25] A. Bogomolova, E. Komarova, K. Reber, T. Gerasimov, O. Yavuz, S. Bhatt, M. Aldissi, Anal. Chem. 81 (2009) 3944.
[26] R. Khan, M. Dhayal, Biosens. Bioelectron. 24 (2009) 1700.
[27] O.V. Gnedenko, Y.V. Mezentsev, A.A. Molnar, A.V. Lisitsa, A.S. Ivanov, A.I. Archakov, Anal. Chim. Acta 759 (2013) 105.
[28] V. Rajesh, V.K. Sharma, S.K. Tanwar, A.M. Mishra, Biradar, Thin Solid Films 519 (2010) 1167.
[29] A.J. Bard, L.R. Faulkner, Electrochemical Methods, John Wiley, New York, 2000.
[30] N. Chauhan, A. Singh, J. Narang, S. Dahiya, C.S. Pundir, Analyst 137 (2012) 5113.
[31] Y. Furkan, C. Emre, S. Mehmet, B. Abdulhadi, Nano-Micro Lett. 3 (2011) 91.
[32] L. Liu, Y. Qin, Z.-X. Guo, D. Zhu, Carbon 41 (2003) 331.
[33] M. Moyo, J.O. Okonkwo, N.M. Agyei, Enzym. Microb. Technol. 56 (2014) 28.
[34] A. Periyakaruppan, R.P. Gandhiraman, M. Meyyappan, J.E. Koehne, Anal. Chem. 85 (2013) 3858.
[35] C.M. Hanbury, W.G. Miller, R.B. Harris, Clin. Chem. 43 (1997) 2128.
[36] F.S. Apple, R.H. Christenson, R. Valdes Jr., A.J. Andriak, A. Berg, S.H. Duh, Y.J. Feng, S.A. Jortani, N.A. Johnson, B. Koplen, K. Mascotti, A.H.B. Wu, Clin. Chem. 45 (1999) 199.
[37] M. Panteghini, Am. J. Clin. Pathol. 118 (2002) 354.
[38] J. Noronha, F.T.C. Moreira, R.F. Dutra, M.G.F. Sales, Electrochim. Acta 107 (2013) 481.
[39] Q. Wang, W. Liu, Y. Xing, X. Yang, K. Wang, R. Jiang, P. Wang, Q. Zhao, Anal. Chem. 86 (2014) 6572.